Discrete Multiwindow Gabor-Type Transforms

Meir Zibulski, *Member, IEEE*, and Yehoshua Y. Zeevi

***Abstract*— The discrete (finite) Gabor scheme is generalized by incorporating multiwindows. Two approaches are presented for the analysis of the multiwindow scheme: the signal domain approach and the Zak transform domain approach. Issues related to undersampling, critical sampling, and oversampling are considered. The analysis is based on the concept of frames and on generalized (Moore–Penrose) inverses. The approach based on representing the frame operator as a matrix-valued function is far less demanding from a computational complexity viewpoint than a straightforward matrix algebra in various operations such as the computation of the dual frame. DFT-based algorithms, including complexity analysis, are presented for the calculation of the expansion coefficients and for the reconstruction of the signal in both signal and transform domains. The scheme is further generalized and incorporates kernels other than the complex exponential. Representations other than those based on the dual frame and nonrectangular sampling of the combined space are considered as well. An example that illustrates the advantages of the multiwindow scheme over the single-window scheme is presented.**

I. Introduction

THE GABOR expansion [1] (or the short-time Fourier transform) was found to be very useful in various fields of physics and engineering for the purpose of signal and image processing and analysis. The continuous Gabor scheme was previously generalized to incorporate several window functions as well as kernels other than the complex exponential [2]. In this paper, we examine the discrete-finite case of the multiwindow Gabor-type scheme and consider issues of interest only in the case of the discrete scheme (algorithms, complexity, etc.). Preliminary results were presented in [3].

Throughout the paper, we consider discrete-time signals that are L-periodic, that is, signals that satisfy $f(i+L) = f(i), i \in \mathbb{Z}$. For such signals, given two divisors M, N of L, i.e., $L = N'M = M'N$, where M, N, M', N' are all positive integers, we propose the following scheme of representation:

$$f(i) = \sum_{r=0}^{R-1}\sum_{m=0}^{M-1}\sum_{n=0}^{N-1} c_{r,m,n} g_{r,m,n}(i) \tag{1}$$

Manuscript received December 21, 1995; revised January 15, 1997. This work was supported in part by the Ollendorff Center, the Fund for the Promotion of Research at the Technion, the MAGNET Consortium for Wideband Communication, and the Israeli Ministry of Science. The associate editor coordinating the review of this paper and approving it for publication was Dr. Victor E. DeBrunner.

M. Zibulski was with the Department of Electrical Engineering, Technion—Israel Institute of Technology, Haifa, Israel. He is now with IBM Science and Technology, Haifa, Israel.

Y. Y. Zeevi is with the Department of Electrical Engineering, Technion—Israel Institute of Technology, Haifa, Israel.

Publisher Item Identifier S 1053-587X(97)04224-4.

where for a set of R window functions $\{g_r(i)\}$, we define

$$g_{r,m,n}(i) = g_r(i - mN') \exp\left(2\pi\imath \frac{in}{N}\right) \tag{2}$$

and $\imath \triangleq \sqrt{-1}$. If $R = 1$, we obtain the known discrete single-window scheme [4]. For $N = 1$, we obtain a finite discrete version of multirate filter banks, where each window function corresponds to a different filter. Thus, (1) incorporates the Gabor scheme (single window) and multirate filter banks.

Let $d \triangleq RMN/L$ be the sampling density of the discrete combined space (so-called phase space). We analyze the three categories:

- undersampling—$d < 1$,
- critical sampling—$d = 1$,
- oversampling—$d > 1$,

and consider issues such as the frame property and algorithms for finding the expansion coefficients.

The paper is organized as follows. In Section II, we consider mathematical preliminaries such as frames, generalized inverses, the Zak transform, and vector-valued functions. Section III is devoted to general analysis of the properties of the sequence of representation functions $\{g_{r,m,n}\}$. Section IV presents algorithms for calculating the expansion coefficients and for the reconstruction of the signal and complexity analysis of these algorithms. Particular cases of single-window schemes and nonrectangular sampling of the combined space are considered in Section V. Section VI presents an example of implementation.

II. Preliminaries

A. Notations

Lowercase boldfaced letters denote column vectors and vector-valued functions such as $\boldsymbol{f}, \boldsymbol{g}(i)$, respectively. Capital boldfaced letters denote matrices and matrix-valued functions such as $\boldsymbol{X}, \boldsymbol{G}(i)$, respectively. The notation $(\boldsymbol{G})_{i,k}$ stands for the entries of the matrix $\boldsymbol{G}$ (similar notation for vectors as well). The entries always start from zero. We use $\overline{f}$ to denote the complex conjugate of f and $\boldsymbol{f}^*$ to denote the complex conjugate transpose of a vector $\boldsymbol{f}$ (similarly for matrices). $\mathbb{Z}$ denotes the integers, and for a positive integer N, $i \in \underline{N}$ means $i = 0, 1, \cdots, N-1$.

B. Frames [5], [6] and Generalized Inverses

Definition 1: A sequence $\{x_n\}$ in a Hilbert space H constitutes a *frame* if there exist numbers $0 < A \le B < \infty$ such that for all $f \in H$ we have $A||f||^2 \le \Sigma_n |\langle f, x_n \rangle|^2 \le B||f||^2$

where $\langle \cdot, \cdot \rangle$ denotes the inner product corresponding to the Hilbert space H.

Definition 2: Given a frame $\{x_n\}$ in a Hilbert space H, the *frame operator* $\mathcal{S}$ is defined by $\mathcal{S}f \triangleq \Sigma_n \langle f, x_n \rangle x_n$. [Note that $\langle \mathcal{S}f, f \rangle = \Sigma_n |\langle f, x_n \rangle|^2$.]

Corollary 1:

1) $\{\mathcal{S}^{-1}x_n\}$ is a frame with bounds B^{-1}, A^{-1} called the *dual frame* of $\{x_n\}$.
2) Every $f \in H$ can be represented by either the frame or the dual frame in the following manner:

$$f = \sum_n \langle f, \mathcal{S}^{-1}x_n \rangle x_n = \sum_n \langle f, x_n \rangle \mathcal{S}^{-1}x_n.$$

Unless the frame is a basis, the representation coefficients $\langle f, \mathcal{S}^{-1}x_n \rangle$ are not unique. The choice of the dual frame for computing the representation coefficients yields the minimal energy solution of the representation coefficients [5]. For a finite-dimensional Hilbert space (as is our case), this solution corresponds to the so-called generalized inverse, and the frame property and completeness are identical. Moreover, for finite-dimensional spaces, every sequence is a frame in its own span.

Without loss of generality (in the context of finite dimensional spaces), consider the space of L-dimensional complex-valued vectors $\mathbb{C}^L$. In this case, the issue of frame expansion can be considered in the context of matrix algebra. Let the columns of the matrix $\boldsymbol{X}$ be the vectors of the finite set $\{\boldsymbol{x}_n\}$. ($\boldsymbol{X}$ is not necessarily a square matrix). The inner products of a given signal $\boldsymbol{f}$, which is also a column vector and the set $\{\boldsymbol{x}_n\}$, can be expressed as a column vector $\boldsymbol{X}^*\boldsymbol{f}$, where $*$ stands for the conjugate transpose. A signal comprised of a set of expansion coefficients given by the column vector $\boldsymbol{c}$, and the expansion set $\{\boldsymbol{x}_n\}$ is given by $\boldsymbol{Xc}$. Thus, the frame operator can be expressed as $\mathcal{S}\boldsymbol{f} = \boldsymbol{XX}^*\boldsymbol{f}$. If $\{\boldsymbol{x}_n\}$ constitutes a frame, the matrix $\boldsymbol{XX}^*$ is nonsingular, and the matrix containing the vectors of the dual frame is given by $(\boldsymbol{XX}^*)^{-1}\boldsymbol{X}$. The representation of $\boldsymbol{f}$ by means of the frame $\{\boldsymbol{x}_n\}$, where the expansion coefficients are calculated by means of the corresponding dual frame, is given by

$$\boldsymbol{f} = \boldsymbol{X}[(\boldsymbol{XX}^*)^{-1}\boldsymbol{X}]^*\boldsymbol{f}. \tag{3}$$

The same representation can be achieved by utilizing the Moore–Penrose or generalized inverse of the matrix $\boldsymbol{X}$, which is denoted by $\boldsymbol{X}^\dagger$ [7]. In fact, $\boldsymbol{c} = \boldsymbol{X}^\dagger\boldsymbol{f}$ is the minimal norm least square solution of the equation $\boldsymbol{Xc} = \boldsymbol{f}$. Moreover, if $\boldsymbol{XX}^*$ is nonsingular, $\boldsymbol{X}^\dagger = \boldsymbol{X}^*(\boldsymbol{XX}^*)^{-1}$, which yields (3), and proves that the application of the dual frame is equivalent to utilizing the Moore–Penrose inverse. Furthermore, if $\boldsymbol{XX}^*$ is singular, i.e., $\{\boldsymbol{x}_n\}$ does not constitute a frame for $\mathbb{C}^L$, we can find the best approximation of the signal by means of the Moore–Penrose inverse. Since, in this case, $\{\boldsymbol{x}_n\}$ constitutes a frame in its own span, the best approximation can also be found by means of the dual frame in the subspace spanned by $\{\boldsymbol{x}_n\}$, and the dual frame can be found utilizing the Moore–Penrose inverse of the frame operator. For general finite-dimensional spaces, these facts are summarized in the following Proposition [8], [9].

Proposition 1: Let H be a finite dimensional Hilbert space, and let $\{x_n\}$ be some finite sequence in H. Denote by $\mathcal{S}^\dagger$ the Moore–Penrose inverse of the frame operator $\mathcal{S}$.

1) $\{\mathcal{S}^\dagger x_n\}$ is the dual frame of $\{x_n\}$ in the sub-space spanned by $\{x_n\}$.
2) For $f \in H$, define $f_{ap} = \Sigma_n \langle f, \mathcal{S}^\dagger x_n \rangle x_n$. Then, $||f - f_{ap}||$ is minimal, and the expansion coefficients $\langle f, \mathcal{S}^\dagger x_n \rangle$ are of minimal norm. Moreover, $f_{ap} = \Sigma_n \langle f, x_n \rangle \mathcal{S}^\dagger x_n$.

C. The Finite Zak Transform (FZT)

The FZT of an L-periodic one-dimensional (1-D) signal is defined by [10], [11]

$$(\mathcal{Z}^a f)(i, v) \triangleq \sum_{k=0}^{b-1} f(i + ka) \exp\left(-2\pi\imath\frac{kv}{b}\right) \qquad (i, v) \in \mathbb{Z}^2 \tag{4}$$

where a, b are integers such that $L = ab$. The FZT is a DFT-based transform and, therefore, can be realized using fast algorithms. The FZT satisfies the following properties [11]:

$$(\mathcal{Z}^a f)(i, v + b) = (\mathcal{Z}^a f)(i, v) \tag{5}$$

$$(\mathcal{Z}^a f)(i + a, v) = \exp\left(2\pi\imath\frac{v}{b}\right)(\mathcal{Z}^a f)(i, v). \tag{6}$$

Unless explicitly stated otherwise, we will use the FZT with $a = N, b = M'$. We omit the superscript a and write $(\mathcal{Z}f)(i, v) \triangleq (\mathcal{Z}^N f)(i, v)$.

Denote by $l^2(\mathbb{Z}/L)$ the Hilbert space of L-periodic square-summable 1-D signals with the following inner product

$$\langle f, g \rangle = \sum_{i=0}^{L-1} f(i)\overline{g(i)} \tag{7}$$

where $f, g \in l^2(\mathbb{Z}/L)$. The FZT (4) defines a unitary mapping of $l^2(\mathbb{Z}/L)$ onto $l^2(\underline{N} \times \underline{M'})$. The latter is a Hilbert space of square-summable two-dimensional (2-D) functions with the inner product

$$\langle \mathcal{Z}f, \mathcal{Z}g \rangle = \frac{1}{M'} \sum_{i=0}^{N-1} \sum_{v=0}^{M'-1} (\mathcal{Z}f)(i, v)\overline{(\mathcal{Z}g)(i, v)}. \tag{8}$$

As a consequence, we obtain the inner product preserving property $\langle f, g \rangle = \langle \mathcal{Z}f, \mathcal{Z}g \rangle$. The inverse of the FZT is given by

$$f(i) = \frac{1}{M'} \sum_{v=0}^{M'-1} (\mathcal{Z}f)(i, v), \qquad i \in \mathbb{Z}. \tag{9}$$

D. Vector-Valued Functions

For the problem addressed in this paper, it is natural to define vector-valued functions that express a sort of decimation. Given $f \in l^2(\mathbb{Z}/L)$, define a vector-valued function of size M' as

$$\boldsymbol{f}(i) = [(\boldsymbol{f})_0(i), \cdots, (\boldsymbol{f})_{M'-1}(i)]^T \tag{10}$$

where $(\boldsymbol{f})_k(i) = f(i + kN), k \in \underline{M'}$. Note that it is sufficient to consider only $i \in \underline{N}$. The inner product in the domain of vector-valued functions can be expressed as

$$\langle \boldsymbol{f}, \boldsymbol{g} \rangle = \sum_{i=0}^{N-1} \boldsymbol{g}^*(i)\boldsymbol{f}(i).$$

Clearly, $\langle f, g \rangle = \langle \boldsymbol{f}, \boldsymbol{g} \rangle$.

For the analysis of the Gabor scheme in the case of oversampling, the concept of vector-valued functions is useful also in the ZT domain [12]. A vector-valued function obtained using the piecewise Zak transform (PZT) was introduced for such an analysis. For the discrete scheme, $L = MN' = NM'$. Let $L/(MN) = p/q$, where p, q are relatively prime integers; then, $M'/p = M/q$ is an integer. Based on the definition of the FZT, (4), we define the piecewise finite Zak transform (PFZT) [3] as a vector-valued function of size p

$$\tilde{\boldsymbol{f}}(i,v) = [(\tilde{\boldsymbol{f}})_0(i,v), \cdots, (\tilde{\boldsymbol{f}})_{p-1}(i,v)]^T \tag{11}$$

where

$$(\tilde{\boldsymbol{f}})_k(i,v) \triangleq (\mathcal{Z}f)\left(i, v + k\frac{M'}{p}\right), \qquad k \in \underline{p}. \tag{12}$$

Note that it is sufficient to consider $i \in \underline{N}, v \in \underline{M'/p}$. The vector-valued function $\tilde{\boldsymbol{f}}(i,v)$ belongs to a Hilbert space of vector-valued functions with the inner product

$$\langle \tilde{\boldsymbol{f}}, \tilde{\boldsymbol{g}} \rangle = \frac{1}{M'} \sum_{i=0}^{N-1} \sum_{v=0}^{(M'/p)-1} \tilde{\boldsymbol{g}}^*(i,v)\tilde{\boldsymbol{f}}(i,v). \tag{13}$$

Thus, here too, we obtain the inner product-preserving property $\langle f, g \rangle = \langle \mathcal{Z}f, \mathcal{Z}g \rangle = \langle \tilde{\boldsymbol{f}}, \tilde{\boldsymbol{g}} \rangle$.

III. General Analysis of the Multiwindow Scheme

The properties of the discrete multiwindow Gabor-type scheme are analyzed in two parallel domains: One is the signal domain, and the other one is the transform domain (FZT domain).

A. The Frame Operator

In order to characterize the frame properties of the sequence $\{g_{r,m,n}\}$, we examine the operator

$$\mathcal{S}f = \sum_{r=0}^{R-1} \sum_{m=0}^{M-1} \sum_{n=0}^{N-1} \langle f, g_{r,m,n} \rangle g_{r,m,n}. \tag{14}$$

If the sequence $\{g_{r,m,n}\}$ constitutes a frame, this is clearly the frame operator. The action of the frame operator in the signal domain can be expressed in terms of matrix algebra as (Appendix A):

$$(\mathcal{S}\boldsymbol{f})(i) = \boldsymbol{S}(i)\boldsymbol{f}(i), \qquad i \in \underline{N} \tag{15}$$

where $\boldsymbol{S}(i)$ is a $M' \times M'$ matrix-valued function with elements given by

$$(\boldsymbol{S})_{k,l}(i) = N \sum_{r=0}^{R-1} \sum_{m=0}^{M-1} g_r(i + kN - mN') \cdot \overline{g_r(i + lN - mN')} \tag{16}$$

and $\boldsymbol{f}(i)$ is a vector-valued function of size M', which is defined by (10). The matrix $\boldsymbol{S}(i)$ is self-adjoint and positive semi-definite for each i since by defining an $RM \times M'$ matrix-valued function $\boldsymbol{G}(i)$

$$\boldsymbol{G}(i) = \begin{pmatrix} \boldsymbol{G}_0(i) \\ \vdots \\ \boldsymbol{G}_{R-1}(i) \end{pmatrix} \tag{17}$$

where each $\boldsymbol{G}_r(i)$ is a matrix-valued function of size $M \times M'$ with elements

$$(\boldsymbol{G}_r)_{m,l}(i) = \overline{g_r(i + lN - mN')}$$

we obtain

$$\boldsymbol{S}(i) = N\boldsymbol{G}^*(i)\boldsymbol{G}(i). \tag{18}$$

Note that $\boldsymbol{S}(i+N') = \boldsymbol{S}(i)$, i.e., the entries of $\boldsymbol{S}(i)$ are periodic with period N' when considering $i \in \mathbb{Z}$.

The action of the frame operator in the PFZT domain can be expressed as (Appendix B)

$$(\widetilde{\mathcal{S}\boldsymbol{f}})(i,v) = \tilde{\boldsymbol{S}}(i,v)\tilde{\boldsymbol{f}}(i,v), \qquad i \in \underline{N}, \quad v \in \underline{M'/p} \tag{19}$$

where $\tilde{\boldsymbol{S}}(i,v)$ is a $p \times p$ matrix-valued function with elements given by

$$(\tilde{\boldsymbol{S}})_{k,j}(i,v) = \frac{N}{p} \sum_{r=0}^{R-1} \sum_{l=0}^{q-1} (\mathcal{Z}g_r)(i - lN', v + kM'/p) \cdot \overline{(\mathcal{Z}g_r)(i - lN', v + jM'/p)} \tag{20}$$

and $\tilde{\boldsymbol{f}}(i,v)$ is a vector-valued function of size p, which is defined by (11). As in the signal domain, the matrix $\tilde{\boldsymbol{S}}(i,v)$ is self-adjoint and positive semi-definite for each (i,v) since by defining a $Rq \times p$ matrix-valued function $\tilde{\boldsymbol{G}}(i,v)$

$$\tilde{\boldsymbol{G}}(i,v) = \begin{pmatrix} \tilde{\boldsymbol{G}}_0(i,v) \\ \vdots \\ \tilde{\boldsymbol{G}}_{R-1}(i,v) \end{pmatrix} \tag{21}$$

where each $\tilde{\boldsymbol{G}}_r(i)$ is a matrix-valued function of size $q \times p$ with elements

$$(\tilde{\boldsymbol{G}}_r)_{l,j}(i,v) = \overline{(\mathcal{Z}g_r)(i - lN', v + jM'/p)}$$

we obtain

$$\tilde{\boldsymbol{S}}(i,v) = \frac{N}{p}\tilde{\boldsymbol{G}}^*(i,v)\tilde{\boldsymbol{G}}(i,v). \tag{22}$$

Note that $\tilde{\boldsymbol{S}}(i+N', v) = \tilde{\boldsymbol{S}}(i,v)$, i.e., in the transform domain as well, the matrix $\tilde{\boldsymbol{S}}(i,v)$ is periodic.

B. Frame Bounds and Properties

Based on the representation of the frame operator presented in Section III-A, we present some results for the discrete multiwindow Gabor-type scheme, which are particular cases of some known facts about frame operators [13]. Note that the sequence $\{g_{r,m,n}\}$ constitutes a frame if and only if $A > 0$ (since in this case, $B < \infty$ always).

It is shown in Appendix C that the frame bounds A, B can be derived by calculating the eigenvalues of the matrix-valued function $\boldsymbol{S}(i)$, i.e.,

$$A = \min_{i \in \underline{N}, j \in \underline{M'}} \lambda_j(\boldsymbol{S})(i) \tag{23}$$

$$B = \max_{i \in \underline{N}, j \in \underline{M'}} \lambda_j(\boldsymbol{S})(i) \tag{24}$$

where $\lambda_j(\boldsymbol{S})(i)$ are the eigenvalues of the matrix $\boldsymbol{S}(i)$. Similarly, we obtain in the transform domain

$$A = \min_{i \in \underline{N}, v \in \underline{M'/p}, j \in \underline{p}} \lambda_j(\tilde{\boldsymbol{S}})(i, v) \tag{25}$$

$$B = \max_{i \in \underline{N}, v \in \underline{M'/p}, j \in \underline{p}} \lambda_j(\tilde{\boldsymbol{S}})(i, v) \tag{26}$$

where $\lambda_j(\tilde{\boldsymbol{S}})(i, v)$ are the eigenvalues of the matrix $\tilde{\boldsymbol{S}}(i, v)$. The ratio B/A, which is the so-called condition number, expresses the stability of the representation. Maximum stability is achieved when $B/A = 1$.

The following theorem [8], [9] considers the frame property of the sequence $\{g_{r,m,n}\}$ without explicitly calculating the frame bounds A, B. It is useful only in the cases of critical sampling and oversampling since in the case of undersampling the sequence, $\{g_{r,m,n}\}$ is always incomplete.

Theorem 1: Given $g_r \in l^2(\mathbb{Z}/L), r \in \underline{R}$, and a matrix-valued function $\boldsymbol{S}(i)$ as in (16) [or $\tilde{\boldsymbol{S}}(i, v)$ as in (20)], the sequence $\{g_{r,m,n}\}$ associated with $\{g_r\}$ constitutes a frame if and only if $\det(\boldsymbol{S})(i) \neq 0$ for all $i \in \underline{N}$ (or $\det(\tilde{\boldsymbol{S}})(i, v) \neq 0$ for all $i \in \underline{N}, v \in \underline{M'/p}$).

A frame $\{\psi_n\}$ in a Hilbert space is called a *tight* frame if $A = B$. The frame operator for tight frames $\mathcal{S} = A\mathcal{I}$, where $\mathcal{I}$ is the identity operator, lends itself to the simple reconstruction formula for each $f \in H: f = A^{-1} \Sigma_n \langle f, \psi_n \rangle \psi_n$. The following theorem considers tight frames and the matrix representation of the frame operator.

Theorem 2: Given $g_r \in l^2(\mathbb{Z}/L), r \in \underline{R}$ and a matrix-valued function $\boldsymbol{S}(i)$ as in (16) [or $\tilde{\boldsymbol{S}}(i, v)$ as in (20)], the sequence $\{g_{r,m,n}\}$ associated with $\{g_r\}$ constitutes a tight frame if and only if $\boldsymbol{S}(i) = A\boldsymbol{I}$ (or $\tilde{\boldsymbol{S}}(i, v) = A\boldsymbol{I}$), where $\boldsymbol{I}$ is the identity matrix, and $A = (MN/L) \Sigma_{r=0}^{R-1} ||g_r||^2$.

Proof: For tight frames, the frame operator is $\mathcal{S} = A\mathcal{I}$. In the domain of vector-valued functions, this is clearly equivalent to $\boldsymbol{S}(i) = A\boldsymbol{I}$ (or $\tilde{\boldsymbol{S}}(i, v) = A\boldsymbol{I}$). To calculate the frame bound, we write this condition explicitly

$$N \sum_{r=0}^{R-1} \sum_{m=0}^{M-1} g_r(i + kN - mN') \overline{g_r(i + lN - mN')} = A\delta_{k-l}$$

where $i \in \underline{N}, k, l \in \underline{M'}$, and δ_m denotes the Kronecker delta function. In particular, we have $(k = l = 0)$

$$\sum_{r=0}^{R-1} \sum_{m=0}^{M-1} |g_r(i - mN')|^2 = \frac{A}{N}.$$

Since

$$||g_r||^2 = \sum_{m=0}^{M-1} \sum_{i=0}^{N'-1} |g_r(i - mN')|^2$$

we have

$$\sum_{r=0}^{R-1} ||g_r||^2 = N' \frac{A}{N}$$

and therefore

$$A = \frac{MN}{L} \sum_{r=0}^{R-1} ||g_r||^2. \qquad \square$$

For maximal oversampling rate, $M = N = L, \boldsymbol{S}(i)$ is scalar-valued and, based on (15) and (16), we have

$$(\mathcal{S}f)(i) = f(i) L \sum_{r=0}^{R-1} ||g_r||^2$$

i.e., the sequence $\{g_{r,m,n}\}$ is always a tight frame (for any set of window functions) with the bounds

$$A = B = L \sum_{r=0}^{R-1} ||g_r||^2$$

(the so-called resolution of identity [3]).

If $\{x_n\}$ constitutes a frame, then $\{\mathcal{S}^{-1/2} x_n\}$ constitutes a tight frame with $A = 1$ [14]. This fact can be utilized for the construction of tight frames of the form $\{\mathcal{S}^{-1/2} g_{r,m,n}\}$. Moreover, let $h_r = \mathcal{S}^{-1/2} g_r$. It can then be shown that $\mathcal{S}^{-1/2} g_{r,m,n} = h_{r,m,n}$, i.e., the tight frame is generated by the R window functions $h_r(i)$ (see [14, prop. 4.6] for the single window continuous-time case and [15, sec. 2.8] for the single window discrete-time case). Clearly, $h_r(x)$ can be found by utilizing $\boldsymbol{S}^{-1/2}(i)$ (or $\tilde{\boldsymbol{S}}^{-1/2}(i, v)$).

C. The Dual Frame

According to Corollary 1, if the sequence $\{g_{r,m,n}\}$ constitutes a frame, the expansion coefficients $c_{r,m,n}$, as in (1), can be calculated by means of the dual frame. Let $\{\gamma_{r,m,n}\}$ denote the dual frame of $\{g_{r,m,n}\}$ in $l^2(\mathbb{Z}/L)$. It can be shown [8], [9] that the structure of the dual frame is identical to that of the frame $\{g_{r,m,n}\}$, i.e., it is generated by R window functions $\gamma_r(i)$

$$\gamma_{r,m,n}(i) = \gamma_r(i - mN') \exp\left(2\pi \imath \frac{in}{N}\right). \tag{27}$$

In fact, $\gamma_r = \mathcal{S}^{-1} g_r$ and, in the signal domain of vector-valued functions, the R dual frame window functions can be calculated by the inverse of the matrix $\boldsymbol{S}(i)$

$$\boldsymbol{\gamma}_r(i) = \boldsymbol{S}^{-1}(i) \boldsymbol{g}_r(i). \tag{28}$$

Note that $\boldsymbol{S}^{-1}(i)$ is in fact the inverse of the $M' \times M'$ matrix $\boldsymbol{S}(i)$ for each $i \in \underline{N}$, where i is a parameter. Alternatively, the R windows of the dual frame can be calculated in the transform domain by the inverse of the matrix $\tilde{\boldsymbol{S}}(i, v)$

$$\tilde{\boldsymbol{\gamma}}_r(i, v) = \tilde{\boldsymbol{S}}^{-1}(i, v) \tilde{\boldsymbol{g}}_r(i, v) \tag{29}$$

where $\tilde{\boldsymbol{\gamma}}_r(i, v), \tilde{\boldsymbol{g}}_r(i, v)$ are the PFZT of $\gamma_r(i), g_r(i)$. Note that an explicit solution by means of the elements of $\boldsymbol{S}(i)$ [or $\tilde{\boldsymbol{S}}(i, v)$] can be found for any given M' (or p). (See [16] for an example of $p = 2$ in the transform domain.)

In the case of critical sampling, the matrix-valued function $\boldsymbol{G}(i)$ [or $\tilde{\boldsymbol{G}}(i,v)$] is a square matrix. Therefore, $\boldsymbol{S}^{-1}(i) = (1/N)\boldsymbol{G}^{-1}(i)\boldsymbol{G}^{-1*}(i)$. Since $\boldsymbol{G}(i)$ can be constructed by utilizing the vector-valued functions $\boldsymbol{g}_r(i)$

$$\boldsymbol{G}_r(i) = \begin{pmatrix} \boldsymbol{g}_r^*(i) \\ \vdots \\ \boldsymbol{g}_r^*(i-(M-1)N') \end{pmatrix} \tag{30}$$

where $r \in \underline{R}$, and $\boldsymbol{G}(i)$ as in (17), we obtain for the dual frame window functions

$$\boldsymbol{\gamma}_r(i) = \frac{1}{N}\begin{pmatrix} (\boldsymbol{G}^{-1})_{0,rM}(i) \\ \vdots \\ (\boldsymbol{G}^{-1})_{M'-1,rM}(i) \end{pmatrix}. \tag{31}$$

That is, $\boldsymbol{\gamma}_r(i)$ is equal to the appropriate column (the rMth column) of the matrix-valued function $(1/N)\boldsymbol{G}^{-1}(i)$. Similarly, in the transform domain, $\tilde{\boldsymbol{\gamma}}_r(i)$ is equal to the appropriate column (the rqth column) of the matrix-valued function $(p/N)\tilde{\boldsymbol{G}}^{-1}(i,v)$.

1) Complexity Analysis: Although the windows of the dual frame are usually calculated off-line (and only once), it is interesting to compare the various techniques for this calculation. Such a comparison could be useful when an adaptive scheme is utilized, where the window functions and, hence, the dual frame window functions, are not known. Our comparison is based on counting the number of complex multiplications, which is of the order of the number of flops, for the calculation of the R dual frame window functions. We are not interested in the exact number of computations but in the order of number of computations. Therefore, we assume that L^3 complex multiplications are needed in order to invert a complex square matrix of size L (indeed, it takes $O(L^3)$ to invert such a matrix [17]).

First, we consider the direct approach as presented in Section II-B. By this approach, we should calculate $(\boldsymbol{X}\boldsymbol{X}^*)^{-1}\boldsymbol{x}_r$, where $\boldsymbol{X}$ is an $L \times RMN$ matrix that has the sequence $\{g_{r,m,n}\}$ as its columns, and $\boldsymbol{x}_r$ are column vectors of size L, which correspond to the set $\{g_r\}, r \in \underline{R}$. The calculation of $\boldsymbol{X}\boldsymbol{X}^*$ entails L^2RMN complex multiplications, the inversion of the resulting matrix requires L^3 complex multiplications, and the additional matrix-vector multiplications take RL^2 complex multiplications. Utilizing $d = RMN/L = Rq/p$, the total number of complex multiplications is $L^3(dR+1+R/L)$. As L grows, this algorithm approaches $O(L^3)$.

Second, we consider the signal domain approach as given by (28). Calculating the entries of $\boldsymbol{S}(i)$, $i \in \underline{N}$, as given by (18), entails M'^2RMN complex multiplications, inverting the resulting matrix-valued function requires M'^3N complex multiplications, and the final matrix-vector multiplications takes RM'^2N complex multiplications. Utilizing the notation $M' = L^\alpha$, where $0 \le \alpha \le 1$, the total number of complex multiplications is $L^{1+2\alpha}(d+1+RL^{-\alpha})$. As L grows, this algorithm requires $O(L^{1+2\alpha})$ multiplications.

Finally, we consider the transform domain approach as given by (29). We assume that there is no need to calculate the inverse FZT of the dual frame window functions since, as we shall see later, the calculations of the expansion coefficients can be done in the transform domain. Calculating the number of complex multiplications in a way similar to the one presented for the signal domain, the total number of complex multiplications is $pRqL+p^2L+RpL$, which is equal to $p^2L(d+1+R/p)$. Assuming that p does not depend on L, as L grows, the complexity of this algorithm becomes $O(L)$.

In summary, for large values of L, the transform domain approach is far less demanding than the other two approaches. Note, however, that if the window functions are all real-valued (which is so in practice), the signal domain approach requires only real operations, which is not true for the transform domain approach. In addition, note that in the case of critical sampling, calculating the dual frame window functions based on $(1/N)\boldsymbol{G}^{-1}(i)$ or $(p/N)\tilde{\boldsymbol{G}}^{-1}(i,v)$ does not change the order of computation complexity.

D. Generalized Inverse and Undersampling

Recall that by utilizing the Moore–Penrose or generalized inverse, we obtain the minimal norm least square solution to a representation problem in finite-dimensional spaces. In our case, if $\{g_{r,m,n}\}$ does not constitute a frame, we can use the Moore–Penrose inverse in order to find the minimal norm coefficients for which expansion of type (1) gives the best approximation of a given signal. As noted, the coefficients can be found by means of the Moore–Penrose inverse of the frame operator

$$c_{r,m,n} = \langle f, \mathcal{S}^\dagger g_{r,m,n}\rangle.$$

The structure of the sequence $\{\mathcal{S}^\dagger g_{r,m,n}\}$, which is the dual frame of $\{g_{r,m,n}\}$ in its own span, is, as expected, identical to the structure of $\{g_{r,m,n}\}$. That is, let $\gamma_{r,m,n} = \mathcal{S}^\dagger g_{r,m,n}$; then, (27) holds, where $\gamma_r = \mathcal{S}^\dagger g_r$. Moreover, the calculation of γ_r can be made similarly to (28), where $\boldsymbol{S}^{-1}(i)$ should be replaced by $\boldsymbol{S}^\dagger(i)$, or, similarly, to (29), where $\tilde{\boldsymbol{S}}^{-1}(i,v)$ should be replaced by $\tilde{\boldsymbol{S}}^\dagger(i,v)$. Furthermore, let $\boldsymbol{\Gamma}(i)$ $(\tilde{\boldsymbol{\Gamma}}(i,v))$ be a matrix-valued function associated with the set $\{\gamma_r\}$ in the same manner as $\boldsymbol{G}(i)$ $(\tilde{\boldsymbol{G}}(i,v))$ is associated with the set $\{g_r\}$. Based on the previous results and on the structure of these matrix-valued functions, we have $\boldsymbol{\Gamma}^*(i) = \boldsymbol{S}^\dagger(i)\boldsymbol{G}^*(i)$. Since $\boldsymbol{G}^\dagger = (\boldsymbol{G}^*\boldsymbol{G})^\dagger\boldsymbol{G}^*$ [7, Theorem 1.2.1], this implies

$$\boldsymbol{\Gamma}^*(i) = \frac{1}{N}\boldsymbol{G}^\dagger(i) \tag{32}$$

or, in the transform domain

$$\tilde{\boldsymbol{\Gamma}}^*(i,v) = \frac{p}{N}\tilde{\boldsymbol{G}}^\dagger(i,v). \tag{33}$$

Equations (32) and (33) present an algorithm, which can be applied in *all possible cases*, for finding the dual frame window functions in the subspace spanned by the $\{g_{r,m,n}\}$.

As indicated by Theorem 1, the frame property of the sequence $\{g_{r,m,n}\}$ can be determined by examining det $(\boldsymbol{S})(i)$ (or det $(\tilde{\boldsymbol{S}})(i,v)$). If the sequence $\{g_{r,m,n}\}$ does not constitute a frame, the dimension of the space spanned by the sequence $\{g_{r,m,n}\}$ can be calculated by examining the matrix-valued function $\boldsymbol{G}(i)$ [or $\tilde{\boldsymbol{G}}(i,v)$], as shown in the following theorem.

Theorem 3: Given $g_r \in l^2(\mathbb{Z}/L), r \in \underline{R}$, and a matrix-valued function $\boldsymbol{G}(i)$ as in (17) [or $\tilde{\boldsymbol{G}}(i,v)$ as in (21)], the dimension of the space spanned by the sequence $\{g_{r,m,n}\}$ associated with $\{g_r\}$ is equal to $\Sigma_{i=0}^{N-1} \operatorname{rank}(\boldsymbol{G})(i)$ [or to $\Sigma_{i=0}^{N-1} \Sigma_{v=0}^{M'/p-1} \operatorname{rank}(\tilde{\boldsymbol{G}})(i,v)$].

Recall that the dimension of a space is the minimum number of representation functions (vectors) required to span the space.

Proof: One can easily verify that span $\{g_{r,m,n}\} = R(\mathcal{S})$, where $\mathcal{S}$ is the frame operator, and $R(\mathcal{S})$ is the range (image) of $\mathcal{S}$. Clearly, the dimension of $R(\mathcal{S})$ can be calculated in the signal domain of vector-valued functions. Since in the signal domain of vector-valued functions the representation of the frame operator is given by the matrix-valued function $\boldsymbol{S}(i)$, which can be represented as in (18), the result in the signal domain follows from matrix algebra considerations. Similarly, based on (22), the result follows also in the transform domain. □

As a matter of fact, in the cases of critical sampling and oversampling, we would like to design the sequence $\{g_{r,m,n}\}$, i.e., choose the window functions g_r such that the sequence constitutes a frame (or a basis) and the reconstruction are perfect. In the case of undersampling, we have no other choice but to utilize the Moore–Penrose inverse in order to get the reconstruction error as small as possible. Moreover, given an undersampling scheme, we would like the $\{g_{r,m,n}\}$ to constitute a basis of a subspace of $l^2(\mathbb{Z}/L)$, i.e., choose the window functions g_r such that the $g_{r,m,n}$ are linearly independent. This basis property is examined in the next theorem through the introduction of the following matrix-valued functions:

$$\boldsymbol{P}(i) = N\boldsymbol{G}(i)\boldsymbol{G}^*(i) \tag{34}$$

where $\boldsymbol{G}(i)$ is as in (17), and

$$\tilde{\boldsymbol{P}}(i,v) = \frac{N}{p}\tilde{\boldsymbol{G}}(i,v)\tilde{\boldsymbol{G}}^*(i,v) \tag{35}$$

where $\tilde{\boldsymbol{G}}(i,v)$ is as in (21).

Theorem 4: Given $g_r \in l^2(\mathbb{Z}/L), r \in \underline{R}$ and a matrix-valued function $\boldsymbol{P}(i)$ as in (34) [or $\tilde{\boldsymbol{P}}(i,v)$ as in (35)], in the case of undersampling, the sequence $\{g_{r,m,n}\}$ associated with $\{g_r\}$ constitutes a basis for a subspace of $l^2(\mathbb{Z}/L)$ if and only if $\det(\boldsymbol{P})(i) \neq 0$ for all $i \in \underline{N}$ [or $\det(\tilde{\boldsymbol{P}})(i,v) \neq 0$ for all $i \in \underline{N}, v \in \underline{M'/p}$].

Proof: In the case of undersampling, the sequence $\{g_{r,m,n}\}$ constitutes a basis of its own span, if and only if the dimension of the space spanned by the sequence $\{g_{r,m,n}\}$ is equal to the number of representation functions in the sequence, i.e., to RNM. Recall that $\boldsymbol{G}(i)$ is of size $RM \times M'$ [and $\tilde{\boldsymbol{G}}(i,v)$ is of size $Rq \times p$] and that in the case of undersampling, $M' > RM$ $(p > Rq)$. Therefore, based on Theorem 3 and (34) [or (35)], the dimension of the space spanned by the sequence $\{g_{r,m,n}\}$ is equal to RNM if and only if $\boldsymbol{P}(i)$ [or $\tilde{\boldsymbol{P}}(i,v)$] is of full rank for each i [or each (i,v)]. □

Note that in case $\{g_{r,m,n}\}$ constitutes a basis in its own span, we have the following formulae for the calculation of the Moore–Penrose inverse [7, Th. 1.3.2]

$$\boldsymbol{S}^\dagger(i) = N\boldsymbol{G}^*(i)\boldsymbol{P}^{-1}(i)\boldsymbol{P}^{-1}(i)\boldsymbol{G}(i)$$

and

$$\tilde{\boldsymbol{S}}^\dagger(i,v) = \frac{N}{p}\tilde{\boldsymbol{G}}^*(i,v)\tilde{\boldsymbol{P}}^{-1}(i,v)\tilde{\boldsymbol{P}}^{-1}(i,v)\tilde{\boldsymbol{G}}(i,v). \tag{36}$$

Moreover, since $\boldsymbol{G}(i)$ can be constructed by utilizing the vector-valued functions $\boldsymbol{g}_r(i)$ as in (30), each dual frame (basis) window function $\boldsymbol{\gamma}_r(i)$ is equal to the appropriate column (the rMth column) of the matrix-valued function $\boldsymbol{G}^*(i)\boldsymbol{P}^{-1}(i)$. Similarly, in the transform domain, $\tilde{\boldsymbol{\gamma}}_r(i)$ is equal to the appropriate column (the rqth column) of the matrix-valued function $\tilde{\boldsymbol{G}}^*(i,v)\tilde{\boldsymbol{P}}^{-1}(i,v)$.

The case where $\{g_{r,m,n}\}$ constitutes an orthonormal basis in its own span can be characterized also by utilizing the matrix-valued functions $\boldsymbol{P}(i), \tilde{\boldsymbol{P}}(i,v)$. The following theorem, which is proved in Appendix D, presents such a characterization.

Theorem 5: Given $g_r \in l^2(\mathbb{Z}/L), r \in \underline{R}$ and a matrix-valued function $\boldsymbol{P}(i)$ as in (34) [or $\tilde{\boldsymbol{P}}(i,v)$ as in (35)], in the case of undersampling, the sequence $\{g_{r,m,n}\}$ associated with $\{g_r\}$ constitutes an orthonormal basis for a subspace of $l^2(\mathbb{Z}/L)$ if and only if $\boldsymbol{P}(i) = \boldsymbol{I}$ [or $\tilde{\boldsymbol{P}}(i,v) = \boldsymbol{I}$], where $\boldsymbol{I}$ is the identity matrix.

E. Representations Other Than the Dual Frame

In the case of oversampling, the expansion coefficients are not unique. As noted, the dual frame provides the coefficients that are of minimal energy in the l^2 sense. We can find, however, different coefficients that still satisfy (1) by calculating the inner products of the signal with sequences $\{\gamma_{r,m,n}\}$ generated by different dual window functions that are not the dual frame window functions. (See [4] and [18] for an example in the single-window case.)

Let $\{\gamma_r\}$ be some given set of R functions. Compute

$$h = \sum_{r=0}^{R-1}\sum_{m=0}^{M-1}\sum_{n=0}^{N-1}\langle f, \gamma_{r,m,n}\rangle g_{r,m,n}$$

where $f(i)$ is some given signal. Based on Appendices A and B, with some minor changes, we obtain, in the domain of vector-valued functions

$$\boldsymbol{h}(i) = N\boldsymbol{G}^*(i)\boldsymbol{\Gamma}(i)\boldsymbol{f}(i) \tag{37}$$

or in the transform domain

$$\tilde{\boldsymbol{h}}(i,v) = \frac{N}{p}\tilde{\boldsymbol{G}}^*(i,v)\tilde{\boldsymbol{\Gamma}}(i,v)\tilde{\boldsymbol{f}}(i,v). \tag{38}$$

Theorem 6: Let $\{g_r\}, \{\gamma_r\}$ be two given sets of R functions each. Then

$$f = \sum_{r=0}^{R-1}\sum_{m=0}^{M-1}\sum_{n=0}^{N-1}\langle f, \gamma_{r,m,n}\rangle g_{r,m,n} \tag{39}$$

for all $f \in l^2(\mathbb{Z}/L)z$ if and only if

$$N\boldsymbol{G}^*(i)\boldsymbol{\Gamma}(i) = \boldsymbol{I}, \quad \left(\frac{N}{p}\tilde{\boldsymbol{G}}^*(i,v)\tilde{\boldsymbol{\Gamma}}(i,v) = \boldsymbol{I}\right). \tag{40}$$

The proof follows (37), (38) (see [19] for the case of a single window). Note that a necessary condition to satisfy (40) is that both $\{g_{r,m,n}\}$ and $\{\gamma_{r,m,n}\}$ constitute frames (not necessarily the dual frame of each other) since both $\boldsymbol{G}(i), \boldsymbol{\Gamma}(i)$ should be of full rank for each i [20].

Given a sequence $\{g_{r,m,n}\}$ that constitutes a frame, i.e., $\boldsymbol{G}(i)$ is of full rank for each i, one of the possible solutions for $\boldsymbol{\Gamma}(i)$ that satisfy (40) is the Moore–Penrose inverse of $N\boldsymbol{G}^*(i)$. Clearly, this solution corresponds to the dual frame of $\{g_{r,m,n}\}$. It is well known that the Moore–Penrose inverse is of minimal Frobenius norm among all possible solutions. This implies that the sum

$$\sum_{r=0}^{R-1}\sum_{m=0}^{M-1}\sum_{l=0}^{M'-1}|\gamma_r(i+lN-mN')|^2$$

attains its minimum for each i if $\{\gamma_{r,m,n}\}$ is the dual frame of $\{g_{r,m,n}\}$. Therefore, among all possible sets $\{\gamma_r\}$ that satisfy (39), the window functions of the dual frame are of minimal norm. (See [15], [21], [22] for the case of a single window.)

F. Representation Functions with Nonexponential Kernels

The representation functions $\{g_{r,m,n}\}$ defined by (2) are constructed by utilizing the complex exponential kernel. This kernel is not the most suitable for all possible applications. For example, for data compression purposes, the cosine kernel might be more attractive. We therefore present and analyze a scheme with kernels that are not necessarily exponential. The case of a continuous-time single-window scheme with critical sampling was introduced in [23].

A general expansion scheme without necessarily having an exponential kernel is based on (1), with the sequence $\{g_{r,m,n}\}$ replaced by the sequence $\{g^{\phi}_{r,m,n}\}$

$$g^{\phi}_{r,m,n}(i) = g_r(i-mN')\phi_n(i). \qquad (41)$$

Each of the functions $\phi_n(i)$ is N periodic, and the sequence $\{(1/\sqrt{N})\phi_n\}$ constitutes an orthonormal basis for $l^2(\mathbb{Z}/N)$. Note that (without loss of generality) we multiply $\phi_n(i)$ by $1/\sqrt{N}$, although we can multiply by any other constant.

This generalization does not change the frame properties of the sequence as shown by the following theorem.

Theorem 7: Let the sequence $\{(1/\sqrt{N})\phi_n\}_{n=0}^{N-1}$ be an N-periodic orthonormal basis for $l^2(\mathbb{Z}/N)$. Then, the sequence $\{g_{r,m,n}\}$ as in (2) and the sequence $\{g^{\phi}_{r,m,n}\}$ as in (41) have the same frame operator $\mathcal{S}$.

Proof: Since $\phi_n(i)$ are N periodic, in the signal domain of vector-valued functions, we have

$$\begin{aligned}(\boldsymbol{g}^{\phi}_{r,m,n})_k(i) &= g^{\phi}_{r,m,n}(i+kN)\\ &= g_r(i+kN-mN')\phi_n(i).\end{aligned} \qquad (42)$$

Examining the derivation of the matrix-valued function $\boldsymbol{S}(i)$ as given in Appendix A, based on (42), it is easily seen that one gets the same matrix $\boldsymbol{S}(i)$ if $\{\exp(2\pi\imath(in/N))\}$ is replaced by $\{\phi_n(i)\}$. □

Note that the operator $\mathcal{S}$ is the same for the two sequences, even when $\{g_{r,m,n}\}$ does not constitute a frame.

As a consequence of Theorem 7, we obtain the following corollary.

Corollary 2: Let the sequence $\{g_{r,m,n}\}$ be as in (2) and the sequence $\{g^{\phi}_{r,m,n}\}$ be as in (41), where $\{(1/\sqrt{N})\phi_n\}_{n=0}^{N-1}$ constitutes an orthonormal basis for $l^2(\mathbb{Z}/N)$.

1) The sequence $\{g_{r,m,n}\}$ is a frame/a tight frame/a basis/an orthonormal basis if and only if the same is true for the sequence $\{g^{\phi}_{r,m,n}\}$.
2) If $\{g_{r,m,n}\}$ constitutes a frame, then $\{g^{\phi}_{r,m,n}\}$ constitutes a frame with the same frame bounds.
3) Let $\{g^{\phi}_{r,m,n}\}$ be a frame with the dual frame $\{\gamma^{\phi}_{r,m,n}\}$. Then, the dual frame is generated by the R functions $\gamma_r = \mathcal{S}^{-1}g_r$, i.e., $\gamma^{\phi}_{r,m,n}(i) = \gamma_r(i-mN')\phi_n(i)$.

Proof: The proof of 1) and 2) is obvious based on the matrix representation of the frame operator. The proof of 3) is similar to the proof of (27). □

IV. Algorithms

The analysis and synthesis of a signal can be done in either the signal or the transform domains. Efficient analysis and synthesis algorithms in the transform domain were presented for a single window and critical sampling in [10] and [11] and were generalized for the case of oversampling [3].

In order to evaluate the complexity, we count only the number of complex multiplications and assume that a 1-D or 2-D DFT of a signal of size L requires $L\log_2 L$ complex multiplications. (For complexity analysis in the case of critical sampling and a single window, see [24].)

A. Calculating the Expansion Coefficients (Analysis)

The expansion coefficients are found by

$$c_{r,m,n} = \langle f, \gamma_{r,m,n}\rangle = \langle \mathcal{Z}f, \mathcal{Z}\gamma_{r,m,n}\rangle. \qquad (43)$$

In the signal domain of vector-valued functions, we have

$$c_{r,m,n} = \sum_{i=0}^{N-1}\left[\sum_{k=0}^{M'-1} f(i+kN)\overline{\gamma_r(i+kN-mN')}\right] \cdot \exp\left(-2\pi\imath\frac{in}{N}\right) \qquad (44)$$

which yields the following DFT-based algorithm for calculating the expansion coefficients:

1) Precompute the dual frame window functions $\gamma_r(i)$.
2) For each $r \in \underline{R}, m \in \underline{M}$, execute the following computations:
   a) For $i \in \underline{N}$, compute $h(i) = \Sigma_{k=0}^{M'-1} f(i+kN)\overline{\gamma_r(i+kN-mN')}$.
   b) Compute a 1-D DFT of length N of $h(i)$.
3) End.

Without counting the stage of precomputing the dual frame window functions, the number of complex multiplications is $RMN(M' + \log_2 N)$. Note that If $M \gg N$, a similar algorithm can be utilized in the Fourier domain, i.e., by considering a 1-D DFT of size L of the functions $g_{r,m,n}(i)$. This, in fact, will exchange the roles of N, M and the roles of N', M' in the complexity computation in addition to a DFT of size L of the signal.

In the transform domain, since

$$(\mathcal{Z}\gamma_{r,m,n})(i,v) = (\mathcal{Z}\gamma_r)(i - mN', v)\exp\left(2\pi\imath\frac{in}{N}\right)$$

we obtain

$$c_{r,m,n} = \frac{1}{M'}\sum_{i=0}^{N-1}\sum_{v=0}^{M'-1}(\mathcal{Z}f)(i,v) \cdot \overline{(\mathcal{Z}\gamma_r)(imN', v)\exp\left(2\pi\imath\frac{in}{N}\right)}. \tag{45}$$

For

$$m = m'q + k, \qquad k \in \underline{q}, \quad m' \in \underline{M'/p}, \quad (M'/p = M/q)$$

by reordering

$$v = v' + jM'/p, \quad v' \in \underline{M'/p}, \qquad j \in \underline{p}$$

(45) can be rewritten as

$$c_{r,m'q+k,n} = \frac{1}{M'}\sum_{i=0}^{N-1}\sum_{v=0}^{(M'/p)-1}\exp\left(-2\pi\imath\frac{in}{N}\right)\exp\left(2\pi\imath\frac{vm'}{M'/p}\right) \cdot \sum_{j=0}^{p-1}(\mathcal{Z}f)\left(i, v + j\frac{M'}{p}\right)\overline{\left(\mathcal{Z}\gamma_r)(i - kN', v + j\frac{M'}{p}\right)} \tag{46}$$

which yields the following DFT-based algorithm for calculating the expansion coefficients:

1) Precompute the FZT of the dual frame window functions $(\mathcal{Z}\gamma_r)(i,v)$.
2) Compute the FZT of the signal $(\mathcal{Z}f)(i,v)$.
3) For each $r \in \underline{R}, k \in \underline{q}$, execute the following steps:
   a) For $i \in \underline{N}, v \in \underline{M'/p}$, compute
   $$h(i,v) = \sum_{j=0}^{p-1}(\mathcal{Z}f)\left(i, v + j\frac{M'}{p}\right) \cdot \overline{(\mathcal{Z}\gamma_r)\left(i - kN', v + j\frac{M'}{p}\right)}.$$
   b) Compute a 2-D DFT of size $N \times M'/p$ of $h(i,v)$.
4) End.

Considering the DFT nature of the FZT, the number of complex multiplications needed in order to calculate $(\mathcal{Z}f)(i,v)$ is $NM'\log_2 M'$. Therefore, without counting the stage of precomputing the dual frame window functions, the total number of complex multiplications is $NM'\log_2 M' + Rq(NM' + NM'/p\log_2(NM'/p))$, which is also equal to $L\log_2 M' + RMN(p - \log_2 p + \log_2 L)$.

The transform domain algorithm is, in fact, a simple generalization of the algorithm presented in [3]. Utilizing $\mathcal{Z}^{N'}$, we present in [8] and [9] another dual algorithm in the transform domain. The complexity of the dual algorithm is essentially the same.

B. Reconstructing the Signal (Synthesis)

The reconstruction of the function from its expansion coefficients is given by (1). In the domain of vector-valued functions, after rearranging the order of summation, we obtain

$$f(i + kN) = \sum_{r=0}^{R-1}\sum_{m=0}^{M-1} g_r(i + kN - mN')\sum_{n=0}^{N-1} c_{r,m,n} \cdot \exp\left(2\pi\imath\frac{in}{N}\right) \tag{47}$$

which yields the following DFT-based reconstruction algorithm:

1) For $r \in \underline{R}, m \in \underline{M}$, compute a 1-D DFT of length N of $c_{r,m,n}$.
2) For $k \in \underline{M'}, i \in \underline{N}$, compute $\Sigma_{r=0}^{R-1}\Sigma_{m=0}^{M-1} g_r(i + kN - mN')\,\mathrm{DFT}\,[c_{r,m,n}]$.

The number of complex multiplications is

$$RMN\log_2 N + M'RMN = RMN(M' + \log_2 N).$$

In the transform domain, the reconstruction of the function is given by

$$(\mathcal{Z}f)(i,v) = \sum_{r=0}^{R-1}\sum_{m=0}^{M-1}\sum_{n=0}^{N-1} c_{r,m,n}(\mathcal{Z}g_r)(i - mN', v) \cdot \exp\left(2\pi\imath\frac{in}{N}\right). \tag{48}$$

Introducing m', k as in (46), for $j \in \underline{p}$, we obtain

$$(\mathcal{Z}f)\left(i, v + j\frac{M'}{p}\right) = \sum_{r=0}^{R-1}\sum_{k=0}^{q-1}(\mathcal{Z}g_r)\left(i - kN', v + j\frac{M'}{p}\right) \cdot \sum_{n=0}^{N-1}\sum_{m'=0}^{(M'/p)-1} c_{r,m'q+k,n}\exp\left(2\pi\imath\frac{in}{N}\right) \cdot \exp\left(-2\pi\imath\frac{vm'}{M'/p}\right) \tag{49}$$

which yields the following DFT-based reconstruction algorithm:

1) Precompute the FZT of the window functions $(\mathcal{Z}g_r)(i,v)$.
2) For $r \in \underline{R}, k \in \underline{q}$, compute a 2-D DFT of size $N \times M'/p$ of $c_{r,m'q+k,n}$.
3) For $j \in \underline{p}, i \in \underline{N}, v \in \underline{M'/p}$, compute
$$\sum_{r=0}^{R-1}\sum_{k=0}^{q-1}(\mathcal{Z}g_r)\left(i - kN', v + j\frac{M'}{p}\right)\mathrm{DFT}\,[c_{r,m'q+k,n}].$$
4) Compute the inverse FZT of $(\mathcal{Z}f)(i,v)$.

The number of complex multiplications is $RqNM'/p\log_2(NM'/p) + NM'Rq + NM'\log_2 M'$, which is equal to $RMN(p - \log_2 p + \log_2 L) + L\log_2 M'$. In this case, as in the case of calculating the expansion coefficients, there exists also a dual algorithm (in the transform domain) that utilizes $\mathcal{Z}^{N'}$.

C. Complexity Comparison

Both analysis and synthesis algorithms require $RMN(M'+\log_2 N)$ complex multiplications in the signal domain. In the transform domain, both algorithms require $RMN(p-\log_2 p+\log_2 L)+L\log_2 M'$ complex multiplications. This can be compared with a straightforward computation of both analysis and synthesis, which requires $RMNL$ complex multiplications. Clearly, in most practical cases, the proposed algorithms perform better than the straightforward calculation. We, therefore, compare only the signal and transform domain algorithms.

Similarly to [24], we write $M' = L^{\alpha}$ and $N = L^{1-\alpha}$, where $0 \leq \alpha \leq 1$. Utilizing $d = RNM/L = Rq/p$, the number of complex multiplications in the signal domain is $dL(L^{\alpha}+(1-\alpha)\log_2 L)$ and in the transform domain is $dL(p-\log_2 p+(\alpha/d+1)\log_2 L)$. In most practical cases, L is large, p is small, $\alpha \approx 0.5$, and d is of an order of a unity. Therefore, roughly speaking, the transform domain algorithm outperforms that of the signal domain in most practical cases. Moreover, assuming that p does not depend on L as L grows, the transform domain algorithm achieves $O(L\log_2 L)$, whereas the signal domain algorithm achieves only $O(L^{1+\alpha})$ (assuming $\alpha \neq 0$). For the single-window case and critical sampling, the fact that the transform domain algorithms achieve the efficiency of an FFT was pointed out in [24].

Clearly, there exists some particular cases where the signal domain algorithms perform better. For example, consider the case of critical sampling. In this case, $d = 1$, and $p = R$. Therefore, if the number of windows is small, the length of the signal is large, and $\alpha \approx 0.5$, the transform domain algorithm outperforms the signal domain algorithm. If the number of windows is large, the two algorithms are of similar complexity, and the specific values of the various parameters should be considered.

V. Examples

A. The Single-Window Scheme

The discrete finite single-window scheme ($R = 1$) was presented in [4], although similar techniques (STFT) were used before [25]. Application of the FZT has been applied in the case of critical sampling [10], [11], and this was generalized to oversampling [3].

The representation scheme in the case of a single window is

$$f(i) = \sum_{m=0}^{M-1}\sum_{n=0}^{N-1} c_{m,n} g_{m,n}(i) \tag{50}$$

where, for the window function $g(i)$, we define

$$g_{m,n}(i) = g(i-mN')\exp\left(2\pi\imath\frac{in}{N}\right), \quad L = N'M. \tag{51}$$

In the case of critical sampling ($L = MN$), $\tilde{\boldsymbol{S}}(i,v) = N|\mathcal{Z}g(i,v)|^2$ is scalar valued. Therefore, there is an advantage in using the FZT. For example, $\{g_{m,n}\}$ constitutes a frame (which is a basis) if and only if $(\mathcal{Z}g)(i,v)$ does not vanish, $\{g_{m,n}\}$ constitutes an orthonormal basis if and only if $N|\mathcal{Z}g(i,v)|^2 = 1$ for all $i \in \underline{N}, v \in \underline{M}$, and the dual frame window is given by $(\mathcal{Z}\gamma)(i,v) = (N\overline{(\mathcal{Z}g)(i,v)})^{-1}$. The computational complexity for calculating the expansion coefficients and for reconstructing the signal is the lowest one in the FZT domain, and it achieves the order of an FFT $O(L\log_2 L)$ [24].

One of the disadvantages of critical sampling is the instability that may occur because of a zero of $(\mathcal{Z}g)(i,v)$ [26], [8]. One solution to this problem is a shift of the window within a subpixel distance [27]. Another is the application of the generalized inverse in order to calculate the best approximation of the signal by the elements of $\{g_{m,n}\}$. Since, in this case, $\tilde{\boldsymbol{S}}(i,v) = N|\mathcal{Z}g(i,v)|^2$ is scalar valued, $\tilde{\boldsymbol{S}}^{\dagger}(i,v) = (\tilde{\boldsymbol{S}}(i,v))^{-1}$ if $\tilde{\boldsymbol{S}}(i,v)) \neq 0$ and $\tilde{\boldsymbol{S}}^{\dagger}(i,v) = 0$ if $\tilde{\boldsymbol{S}}(i,v) = 0$. This implies that the expansion coefficients can be calculated utilizing only the nonzero values of $(\mathcal{Z}g)(i,v)$. (For a different approach that leads to a similar result, see [28].)

A third solution to the problem of instability is to consider an oversampling scheme ($MN > L$), in which case, the FZT plays an important role as well [3]. The effect of oversampling is easily understood in the case of an integer oversampling rate, i.e., for $L/(MN) = 1/q$, where $q > 1$ is an integer. In such a case, $\tilde{\boldsymbol{S}}(i,v)$ is scalar valued

$$\tilde{\boldsymbol{S}}(i,v) = N\sum_{l=0}^{q-1}|(\mathcal{Z}g)(i-lN',v)|^2.$$

Therefore, if $\mathcal{Z}g$ has only a single zero (in a square of size $N \times M'$ in the (i,v) plane), such an oversampling will clearly stabilize the scheme since $\tilde{\boldsymbol{S}}(i,v)$ does not vanish. Moreover, if $\tilde{\boldsymbol{S}}(i,v)$ does vanish, the expansion coefficients that correspond to the generalized inverse solution can be found by utilizing only the nonzero values of $\tilde{\boldsymbol{S}}(i,v)$ similarly to the critical sampling case.

In some cases, there is an advantage in performing the analysis in the signal domain. For example, consider $g(i)$ such that $g(i) = 0$ for $N \leq i \leq L-1$ ($g(i)$ is compactly supported). In such a case, $\boldsymbol{S}(i)$ is diagonal with

$$(\boldsymbol{S})_{k,k}(i) = \sum_{m=0}^{M-1}|g(i+kN-mN')|^2.$$

Therefore, $\{g_{m,n}\}$ constitutes a frame if and only if $(\boldsymbol{S})_{0,0}(i)$ does not vanish for $i \in \underline{N'}$. It is a tight frame if and only if $(\boldsymbol{S})_{0,0}(i)$ is a constant function, and the dual frame is given by

$$\gamma(i) = \frac{g(i)}{\sum_{m=0}^{M-1}|g(i-mN')|^2}.$$

It is interesting to point out the particular case of an integer undersampling rate, i.e., $L/(MN) = p$, where p is an integer. In this case, $\tilde{\boldsymbol{G}}(i,v)$ is of size $1 \times p$, i.e., it is a vector-valued function, and

$$\tilde{\boldsymbol{P}}(i,v) = N/p\sum_{k=0}^{p-1}|(\mathcal{Z}g)(i,v+kM'/p)|^2$$

is scalar valued. In fact, $\tilde{\boldsymbol{G}}(i,v) = \tilde{\boldsymbol{g}}^*(i,v)$. Therefore, if

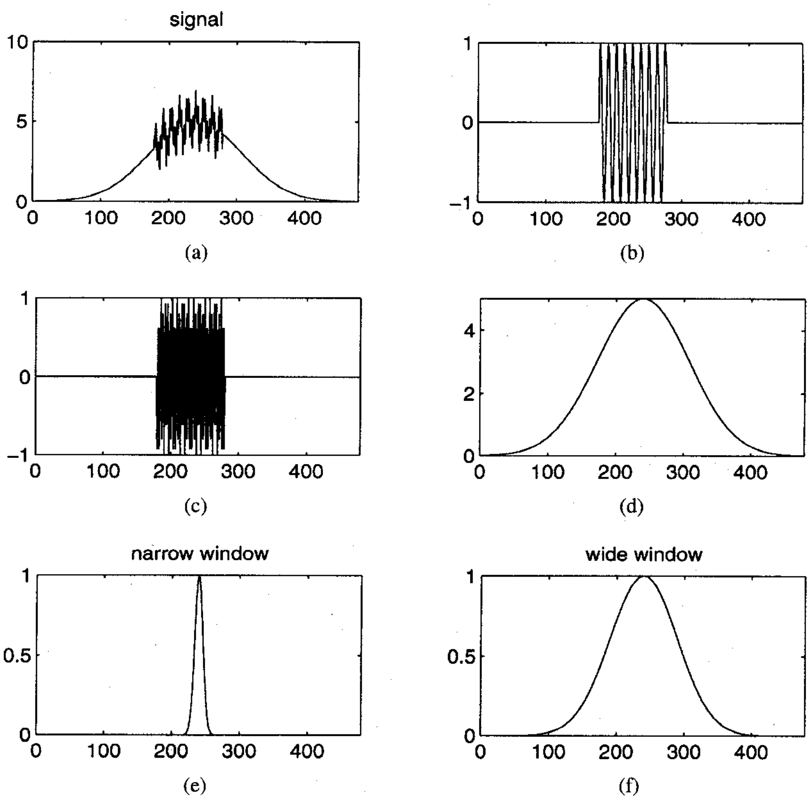

Fig. 1. (a) Signal. (b)–(d) Signal's components. (e) and (f) Narrow and wide windows.

$\{g_{m,n}\}$ constitutes a basis in its own span, i.e., $\tilde{P}(i,v)$ does not vanish, based on (36), the FZT of the window function that generates the dual (biorthonormal) basis is

$$(\mathcal{Z}\gamma)(i,v) = \frac{N(\mathcal{Z}g)(i,v)}{p\sum_{k=0}^{p-1}|(\mathcal{Z}g)(i,v+kM'/p)|^2}. \tag{52}$$

Note that if $\tilde{P}(i,v)$ does vanish, we can still calculate $\tilde{S}^{\dagger}(i,v)$, in which case, the dual frame (a frame in its own span) window function is given by (52) but is zero wherever $\tilde{P}(i,v)$ vanishes. This particular case was analyzed by a different method in [28], yielding a similar solution.

B. Nonrectangular Sampling of the Combined Space

In the case of a single-window scheme, one may view the representation functions $g_{m,n}(i)$ as localized around the points (mN', nM') of the combined discrete finite time-frequency space (phase space) of size $L \times L$. Clearly, the functions defined in (51) represent a rectangular sampling of the combined space (rectangular lattice). Utilizing the scheme of several window functions, one may sample the combined space according to a nonrectangular lattice.

For example, consider a two-window scheme such that $g_0(i) = g(i), g_1(i) = g(i-a)\exp(2\pi\imath(ib/L))$, where $a \in \underline{N'}, b \in \underline{M'}$. Now, the combined space is sampled at the points $(mN', nM') \cup (mN'+a, nM'+b)$. In particular, we may construct a hexagonal lattice [29] by taking $a = N'/2, b = M'/2$ (assuming N', M' is divisible by 2).

A general setting of a nonrectangular sampling, based on a single window function $g(i)$, is based on (1), where the R window functions g_r are defined by

$$g_r(i) = g(i-a_r)\exp\left(2\pi\imath\frac{ib_r}{L}\right) \tag{53}$$

where it is sufficient to consider $a_r \in \underline{N'}, b_r \in \underline{M'}$. We assume that $a_r = a_k, b_r = b_k$ only if $r = k$ and then have

$$g_{r,m,n}(i) = \exp\left(-2\pi\imath\frac{ib_r mN'}{L}\right)g(i-mN'-a_r) \cdot \exp\left(2\pi\imath\frac{i(nM'+b_r)}{L}\right).$$

Based on (16), the elements of the matrix $S(i)$ in the signal domain are

$$(S)_{k,l}(i) = N\sum_{r=0}^{R-1}\exp\left(2\pi\imath\frac{(k-l)b_r}{M'}\right) \cdot \sum_{m=0}^{M-1} g(i-a_r+kN-mN') \cdot \overline{g(i-a_r+lN-mN')}. \tag{54}$$

The elements of the matrix $\tilde{S}(i,v)$ can be easily found based on

$$(\mathcal{Z}g_r)(i,v) = (\mathcal{Z}g)(i-a_r, v-b_r)\exp\left(2\pi\imath\frac{ib_r}{L}\right). \tag{55}$$

In this setting, the sequence $\{g_{r,m,n}\}$ is generated by a single window function. This is not true for the dual frame

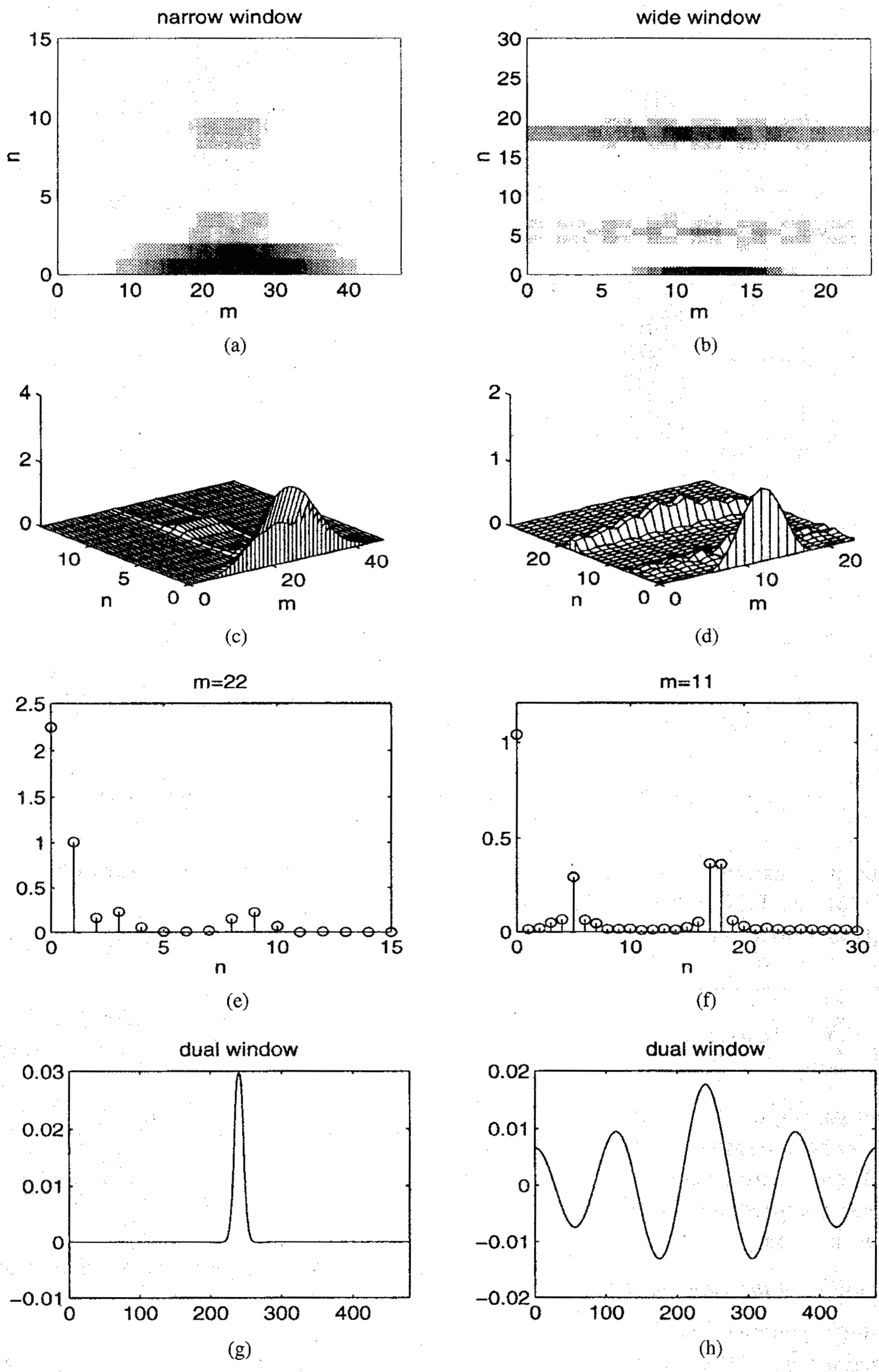

Fig. 2. Single-window schemes. (a) and (b) Gray-level plots of the absolute values of the expansion coefficients corresponding to the narrow and wide windows, respectively. (c) and (d) Corresponding absolute value plots. (e) and (f) Cross-section at $m = 22$ for the narrow window and a cross-section at $m = 11$ for the wide window, respectively. (g) and (h) Dual frame window functions of the narrow and wide windows, respectively.

$\{\gamma_{r,m,n}\}$, except for some particular cases. If

$$a_r = \frac{N'}{R}r, \quad b_r = \frac{M'}{R}r$$

(assuming N', M' are divisible by R), the dual frame is generated by a single window function $\gamma(i)$ [8], [9]

$$\gamma_{r,m,n}(i) = \exp\left(-2\pi\imath\frac{ib_r mN'}{L}\right)\gamma(i - a_r - mN') \cdot \exp\left(2\pi\imath\frac{i(nM' + b_r)}{L}\right). \tag{56}$$

The dual frame window function can be found in the signal domain $\gamma(i) = S^{-1}(i)g(i)$ (or in the transform domain $\tilde{\gamma}(i,v) = \tilde{S}^{-1}(i,v)\tilde{g}(i,v)$).

VI. Example of Implementation

In the case of a multicomponent signal where the components are distinctly characterized in the time-frequency (position-frequency) space, it is not possible to select an optimal window for a single-window scheme. In such cases, it is advantageous to use the multiwindow scheme as is

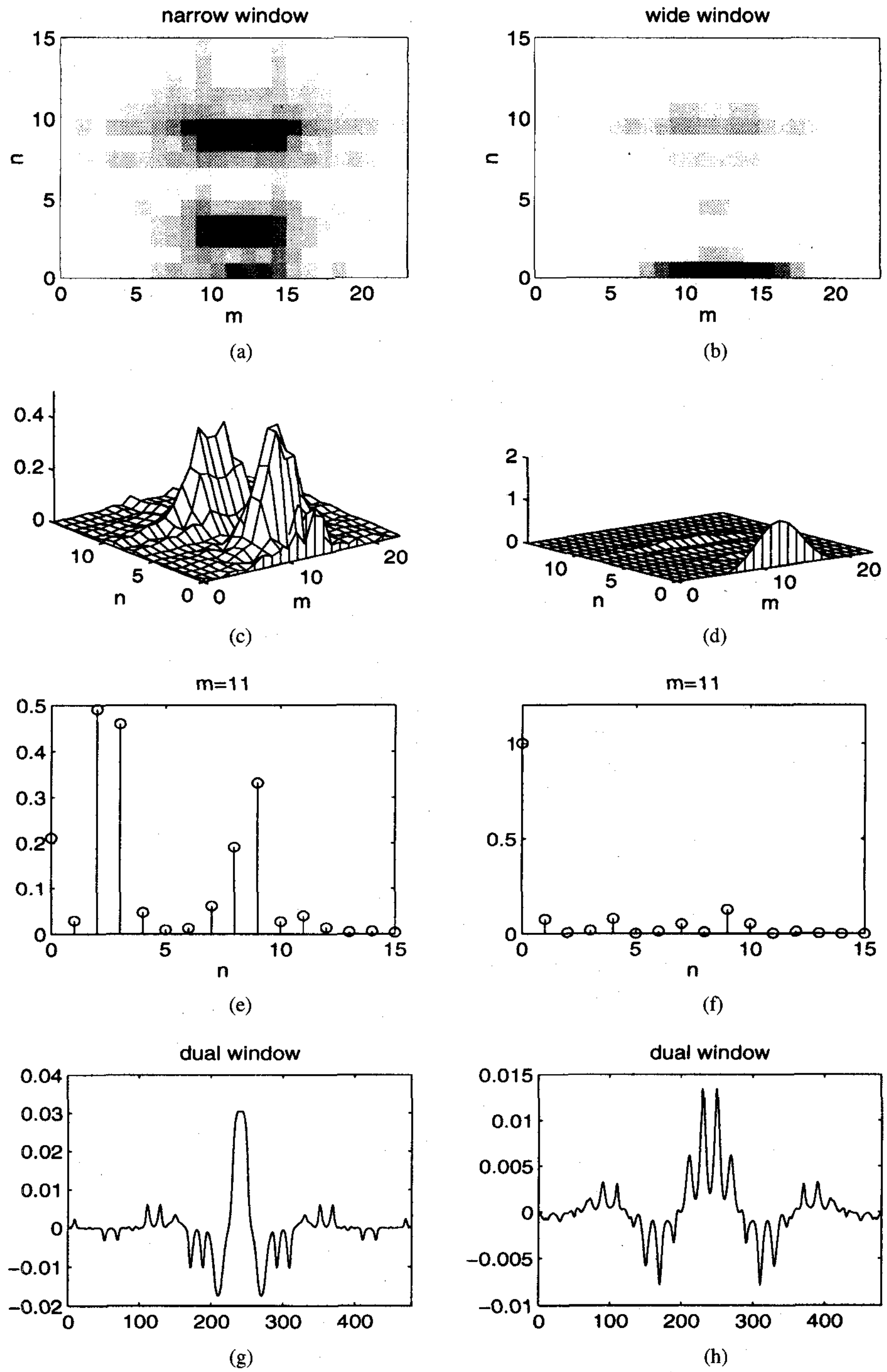

Fig. 3. Double-window scheme. (a) and (b) Gray-level plots of the absolute values of the expansion coefficients corresponding to the narrow and wide windows, respectively. (c) and (d) Corresponding absolute value plots. (e) and (f) Cross-section at $m = 11$ for the narrow and wide windows, respectively. (g) and (h) Dual frame window function for the narrow and wide windows, respectively.

demonstrated by the following example. Consider the signal $f(i)$ [Fig. 1(a)] of length $L = 480$, which is comprised of three different components: $f(i) = f_1(i) + f_2(i) + f_3(i)$. The signals $f_1(i), f_2(i)$ [Fig. 1(b) and (c)] are two time-limited tones overlapping in time. The signal $f_3(t)$ [Fig. 1(d)] is a wide Gaussian envelope.

Three different schemes are utilized in order to analyze the structure of the signal, and their performances are compared. First, we consider a single-window scheme ($R = 1$) with a narrow Gaussian window [Fig. 1(e)] and $M = 48, N = 30, p = 1, q = 3$. Second, we consider a single-window scheme with a wide Gaussian window [Fig. 1(e)], and $M = 24, N = 60, p = 1, q = 3$. Finally, we consider a double-window scheme ($R = 2$) with both the narrow and wide windows, and $M = 24, N = 30, p = 2, q = 3$.

Note that in all three cases, we use the same number of representation functions, whereas the tessellation of the combined space is different. Even in the case of a single window, there is a proper way or even an optimal one to tessellate the combined space once the structure (including width) of a window has been selected with reference to the signals to be analyzed. To be more specific, given a certain sampling density of the combined space, there is a degree of freedom of determining the distribution of the representation functions. However, if the criterion of optimal (minimal) condition number (recall that the condition number is equal to B/A) is to be satisfied, the distribution of the representation functions is dictated by the window. For this reason, in the two cases of the single-window scheme, the distributions are different, whereas in the case of the wide window, there is a high density of representation functions along the frequency axis and low density along the time (position) axis, and in the case of a narrow window, the densities are the other way around. Consequently, in the case of the wide window, there is a high resolution along the frequency axis on the expense of a wide spread along the time (position) axis, which eliminates the temporal (spatial) fine structure of the signal. In the case of the narrow window, the distributions of the functions and resultant resolutions are the other way around. In the case of a multiwindow scheme, the distribution is also dictated by the windows, but the scheme incorporates several degrees of freedom. Therefore, to simplify matters and reduce the number of degrees of freedom, we have limited the analysis to the case of identical overlaying sampling grids of the combined space for all windows. (Note that the distributions do not have to be identical and, in fact, should be different to satisfy some kind of optimality). Based on these restrictions and the fact that the number of representation functions is similar for all schemes, we obtained the distribution for the double-window scheme (the distribution along the frequency axis is similar to the distribution for the narrow single-window scheme, and the distribution along the temporal (spatial) axis is similar to the distribution for the wide single-window scheme).

The absolute values of the expansion coefficients corresponding to the narrow and wide single-window schemes are shown in Fig. 2(c) and (d) respectively, with corresponding gray-level plots shown in Fig. 2(a) and (b), respectively. Cross sections at $m = 22$ ($mN' = 220$) for the narrow window and at $m = 11$ ($mN' = 220$) for the wide window are shown in Fig. 2(e) and (f), respectively. The dual frame windows are shown in Fig. 2(g) and (h) for the narrow and wide windows, respectively. Considering first the narrow window case, Fig. 2 clearly depicts the Gaborian representation of the wide Gaussian envelope, along with some traces of the two tones. Note, however, that the fingerprint of the low-frequency tone is not so clear, i.e., it merges with that of the wide Gaussian envelope (a spread over the frequency axis). In the case of the wide window, one can clearly see the three different frequencies corresponding to the Gaussian envelope and the two tones. However, the temporal (spatial) resolution of the two tones is very poor, i.e., there is a wide spread of the signal, in particular, of the high-frequency tone.

The absolute values of the expansion coefficients of the double-window scheme are shown in Fig. 3(c) [with corresponding gray-level plot in Fig. 3(a)] for the coefficients corresponding to the narrow window and in Fig. 3(d) and (b) for the coefficients corresponding to the wide window. A cross section at $m = 11$ ($mN' = 220$) for the narrow and wide windows is shown in Fig. 3(e) and 3(f), respectively. In addition, the dual frame windows are shown in Fig. 3(g) and (h) for the narrow and wide windows, respectively. It appears as though the multiwindow scheme can, with proper rate of oversampling, overcome in some way the limitations imposed by the uncertainty principle on the simultaneous resolution in time (position) and frequency. In the case of the multiwindow scheme, each of the windows can lock on certain components of the signal if the windows are properly selected. By displaying the components corresponding to the two windows of the above (double-window) example separately, it is observed that this is indeed the case. The broadly tuned (in time) Gaussian component of the signal is clearly captured by the wide window, whereas the two tones are hardly represented (and are smeared in time) by this window. On the other hand, the two tones are clear and localized in the representation of the components corresponding to the narrow window, whereas the broad Gaussian component is hardly represented.

Note the different structure of the dual windows corresponding to the single- and double-window schemes. Clearly, in the double-window scheme, one window is affected by the other (which is not so in the case of the single window). This, in fact, causes the advantages offered by a double-window (multiwindow) scheme. Thus, the processing, signal component separation, and identification obtained by the double-window scheme cannot be obtained by a combination of processing by two single-window schemes.

APPENDIX A
PROOF OF EQUATIONS (15) AND (16)

For vector-valued functions as defined in (10), we have

$$
\begin{aligned}
(\boldsymbol{g}_{r,m,n})_k(i) &= g_{r,m,n}(i+kN)\\
&= g_r(i+kN-mN')\exp\left(2\pi\imath\frac{in}{N}\right).
\end{aligned}
$$

In the domain of vector-valued functions, the kth element $k \in \underline{M'}$ of $\mathcal{S}$ acting on $\boldsymbol{f}$ is

$$
\begin{aligned}
(\mathcal{S}\boldsymbol{f})_k(i) &= \sum_{r=0}^{R-1}\sum_{m=0}^{M-1}\sum_{n=0}^{N-1}\langle \boldsymbol{f}, \boldsymbol{g}_{r,m,n}\rangle(\boldsymbol{g}_{r,m,n})_k(i)\\
&= \sum_{r=0}^{R-1}\sum_{m=0}^{M-1}\sum_{n=0}^{N-1} g_r(i+kN-mN')\exp\left(2\pi\imath\frac{in}{N}\right)\\
&\quad \cdot \sum_{i'=0}^{N-1}\sum_{l=0}^{M'-1}(\boldsymbol{f})_l(i')\overline{g_r(i'+lN-mN')}\\
&\quad \cdot \exp\left(-2\pi\imath\frac{i'n}{N}\right).
\end{aligned}
$$

Since $\{1/\sqrt{N}\exp(2\pi\imath(in/N))\}_n$ constitutes an orthonormal basis for the Hilbert space of square summable finite signals of length N, we have

$$
\begin{aligned}
(\mathcal{S}\boldsymbol{f})_k(i) = N\sum_{r=0}^{R-1}\sum_{m=0}^{M-1}\sum_{l=0}^{M'-1} g_r(i+kN-mN')\\
\cdot (\boldsymbol{f})_l(i)\overline{g_r(i+lN-mN')}
\end{aligned}
$$

which, in terms of matrix algebra, yields (15) and (16).

APPENDIX B
PROOF OF (19) AND (20)

Based on the definition of the FZT (4), it can easily be shown that

$$(\mathcal{Z}g_{r,m,n})(i,v) = (\mathcal{Z}g_r)(i - mN', v)\exp\left(2\pi\imath\frac{in}{N}\right). \quad (57)$$

Let $L/(MN) = p/q$, where p, q are relatively prime integers. It then follows that $M'/p = M/q$ is an integer. For $m = m'q + l, l \in \underline{q}, m' \in \underline{M'/p}$, we have

$$(\mathcal{Z}g_{r,m'q+l,n})(i,v) = (\mathcal{Z}g_r)(i - lN', v)\exp\left(2\pi\imath\frac{in}{N}\right) \cdot \exp\left(-2\pi\imath\frac{m'pv}{M'}\right).$$

In the PFZT domain, the kth element $k \in \underline{p}$ of $\mathcal{S}$ acting on $\tilde{\boldsymbol{f}}(i,v)$ is

$$\begin{aligned}(\mathcal{S}\tilde{\boldsymbol{f}})_k(i,v) =& \sum_{r=0}^{R-1}\sum_{n=0}^{N-1}\sum_{m'=0}^{(M'/p)-1}\sum_{l=0}^{q-1}(\mathcal{Z}g_r)(i-lN', v+kM'/p) \\ &\cdot \exp\left(2\pi\imath\frac{in}{N}\right)\exp\left(-2\pi\imath\frac{m'pv}{M'}\right) \\ &\cdot \frac{1}{M'}\sum_{i'=0}^{N-1}\sum_{v'=0}^{(M'/p)-1}\sum_{j=0}^{p-1}(\tilde{\boldsymbol{f}})_j(i',v') \\ &\cdot \overline{(\mathcal{Z}g_r)(i' - lN', v' + jM'/p)} \\ &\cdot \overline{\exp\left(2\pi\imath\frac{i'n}{N}\right)\exp\left(-2\pi\imath\frac{m'pv'}{M'}\right)}.\end{aligned}$$

Since

$$\{\sqrt{p/(NM')}\exp(2\pi\imath(in/N))\exp(-2\pi\imath(m'pv/M'))\}_{m,n'}$$

constitutes an orthonormal basis for the Hilbert space of square summable 2-D finite signals of size $N \times M'/p$, we have

$$\begin{aligned}(\mathcal{S}\tilde{\boldsymbol{f}})_k(i,v) =& \frac{N}{p}\sum_{r=0}^{R-1}\sum_{l=0}^{q-1}(\mathcal{Z}g_r)(i - lN', v + kM'/p) \\ &\cdot \sum_{j=0}^{p-1}(\tilde{\boldsymbol{f}})_j(i,v)\overline{(\mathcal{Z}g_r)(i - lN', v + jM'/p)}\end{aligned}$$

which in terms of matrix algebra yields (19) and (20).

APPENDIX C
RELATIONS FOR THE FRAME BOUNDS

Let

$$A(i) = \min_j \lambda_j(\boldsymbol{S})(i), \quad B(i) = \max_j \lambda_j(\boldsymbol{S})(i).$$

Since for each $i\boldsymbol{S}(i)$ is self-adjoint and positive semi-definite, we have

$$A(i)\boldsymbol{f}^*(i)\boldsymbol{f}(i) \le \boldsymbol{f}^*(i)\boldsymbol{S}(i)\boldsymbol{f}(i) \le B(i)\boldsymbol{f}(i)^*\boldsymbol{f}(i) \quad (58)$$

for all $\boldsymbol{f}(i)$. Basically, the frame bounds satisfy

$$A = \inf_{||f||=1}\langle \mathcal{S}f, f\rangle, \quad B = \sup_{||f||=1}\langle \mathcal{S}f, f\rangle.$$

Therefore, based on (58) and on

$$\langle \mathcal{S}f, f\rangle = \sum_{i=0}^{N-1}\boldsymbol{f}^*(i)\boldsymbol{S}(i)\boldsymbol{f}(i)$$

we have for the frame bounds

$$A \ge \min_{i\in\underline{N}} A(i) \quad (59)$$

$$B \le \max_{i\in\underline{N}} B(i). \quad (60)$$

To show that equality is obtained in (59), we find a function $f(i)$ for which an equality is satisfied. Let $i_{\min}$ be such that in (23), $A = \lambda_j(i_{\min})$ for some j, i.e., $\lambda_j(i_{\min})$ is the minimum eigenvalue of $\boldsymbol{S}(i_{\min})$. Choose $\boldsymbol{f}(i)$ such that $\boldsymbol{f}(i_{\min})$ is the corresponding normalized eigenvector of the minimum eigenvalue and zero for other values of i. This $\boldsymbol{f}(i)$ satisfies the equality. Similarly, by choosing an appropriate $\boldsymbol{f}(i)$ (corresponding to the maximum eigenvalue), equality in (60) is obtained as well.

APPENDIX D
PROOF OF THEOREM 5

The orthonormality condition is

$$\langle g_{s,k,n}, g_{t,l,n'}\rangle = \delta_{t-s}\delta_{k-l}\delta_{n-n'}$$

where δ_n is the Kronecker delta function. Explicitly, this condition can be written as

$$\sum_{i=0}^{L-1} g_s(i - kN')\overline{g_t(i - lN')}\exp\left(2\pi\imath\frac{in}{N}\right) = \delta_{t-s}\delta_{k-l}\delta_n. \quad (61)$$

Reordering $i = i' + jN, i' \in \underline{N}, j \in \underline{M'}$ (61) becomes

$$\begin{aligned}\sum_{i'=0}^{N-1}\exp\left(2\pi\imath\frac{i'n}{N}\right)&\sum_{j=0}^{M'-1} g_s(i' + jN - kN') \\ &\cdot \overline{g_t(i' + jN - lN')} = \delta_{t-s}\delta_{k-l}\delta_n. \quad (62)\end{aligned}$$

One observes that the left-hand side of (62) involves a DFT of size N. Therefore, performing IDFT on both sides of (62), we obtain the following necessary and sufficient condition for orthonormality:

$$\sum_{j=0}^{M'-1} g_s(i + jN - kN')\overline{g_t(i + jN - lN')} = \delta_{t-s}\delta_{k-l}N^{-1} \quad (63)$$

for all $i \in \underline{N}$.

On the other hand, we calculate the entries of the matrix-valued function $\boldsymbol{P}(i)$. Partition $\boldsymbol{P}(i)$ into blocks in the following manner:

$$\boldsymbol{P}(i) = \begin{pmatrix} \boldsymbol{P}^{0,0}(i) & \cdots & \boldsymbol{P}^{0,R-1}(i) \\ \vdots & & \vdots \\ \boldsymbol{P}^{R-1,0}(i) & \cdots & \boldsymbol{P}^{R-1,R-1}(i)\end{pmatrix}$$

where each block $\boldsymbol{P}^{t,s}(i)$ is a matrix-valued function of size $M \times M$, with entries

$$(\boldsymbol{P}^{t,s})_{l,k}(i) = N \sum_{j=0}^{M'-1} g_s(i + jN - kN')\overline{g_t(i + jN - lN')}.$$

Therefore, $\boldsymbol{P}(i) = \boldsymbol{I}$ is equivalent to (63), which is equivalent to the orthonormality condition. Similarly, one can prove that $\tilde{\boldsymbol{P}}(i, v) = \boldsymbol{I}$, is equivalent to the orthonormality condition. $\square$

References

[1] D. Gabor, "Theory of communication," *J. Inst. Elect. Eng. London*, vol. 93, no. III, pp. 429–457, 1946.

[2] M. Zibulski and Y. Y. Zeevi, "Analysis of multi-window Gabor-type schemes by frame methods," *Applied Comput. Harmonic Anal.*, in press; also in CC Pub. 101, Technion—Israel Inst. Technol., Haifa, Apr. 1995.

[3] ——, "Frame analysis of the discrete Gabor-scheme," *IEEE Trans. Signal Processing*, vol. 42, pp. 942–945, Apr. 1994.

[4] J. Wexler and S. Raz, "Discrete Gabor expansions," *Signal Processing*, vol. 21, pp. 207–220, 1990.

[5] R. J. Duffin and A. C. Schaeffer, "A class of nonharmonic Fourier series," *Trans. Amer. Math. Soc.*, vol. 72, pp. 341–366, 1952.

[6] C. Heil and D. Walnut, "Continuous and discrete wavelet transforms," *SIAM Rev.*, vol. 31, pp. 628–666, 1989.

[7] S. L. Campbell and C. D. Meyer, *Generalized Inverses of Linear Transformations*. London: Pitman, 1979.

[8] M. Zibulski, "Gabor-type representations of signals and images," Ph.D. dissertation, Technion–Israel Inst. Technol., Haifa, Oct. 1995.

[9] M. Zibulski and Y. Y. Zeevi, "Discrete multi-window Gabor-type transforms," CC Pub. 124, Technion—Israel Inst. Technol., Haifa, Nov. 1995.

[10] L. Auslander, I. Gertner, and R. Tolimieri, "The discrete Zak transform application to time-frequency analysis and synthesis of nonstationary signals," *IEEE Trans. Signal Processing*, vol. 39, pp. 825–835, 1991.

[11] Y. Y. Zeevi and I. Gertner, "The finite Zak transform: An efficient tool for image representation and analysis," *J. Visual Comm. Image Represent.*, vol. 3, pp. 13–23, Mar. 1992.

[12] M. Zibulski and Y. Y. Zeevi, "Matrix algebra approach to Gabor-scheme analysis," EE Pub. 856, Technion—Israel Inst. Technol., Haifa, Sept. 1992.

[13] I. Daubechies, *Ten Lectures on Wavelets*. Philadelphia, PA: SIAM, 1992.

[14] D. F. Walnut, "Continuity properties of the Gabor frame operator," *J. Math. Anal. Appl.*, vol. 165, pp. 479–504, 1992.

[15] A. J. E. M. Janssen, "Duality and biorthogonality for discrete-time Weyl-Heisenberg frames," preprint, 1994.

[16] M. Zibulski and Y. Y. Zeevi, "Oversampling in the Gabor scheme," *IEEE Trans. Signal Processing*, vol. 41, pp. 2679–2687, Aug. 1993.

[17] G. W. Stewart, *Introduction to Matrix Computations*. London, U.K.: Academic, 1973.

[18] S. Qian and D. Chen, "Discrete Gabor transform," *IEEE Trans. Signal Processing*, vol. 41, pp. 2429–2438, July 1993.

[19] A. J. E. M. Janssen, "On rationally oversampled Weyl–Heisenberg frames," *Signal Processing*, vol. 47, pp. 239–245, 1995.

[20] P. Lancaster and M. Tismenetsky, *The Theory of Matrices*. Orlando, FL: Academic, 1985.

[21] A. J. E. M. Janssen, "Duality and biorthogonality for Weyl–Heisenberg frames," *J. Fourier Anal. Applications*, vol. 1, pp. 403–436, 1995.

[22] I. Daubechies, H. Landau, and Z. Landau, "Gabor time-frequency lattices and the Wexler-Raz identity," *J. Fourier Anal. Applications*, vol. 1, pp. 437–478, 1995.

[23] P. D. Einziger, S. Raz, and S. Farkash, "Gabor expansion on orthogonal bases," *Electron. Lett.*, vol. 25, pp. 80–82, 1989.

[24] R. S. Orr, "The order of computation for finite discrete Gabor transforms," *IEEE Trans. Signal Processing*, vol. 41, pp. 122–130, 1993.

[25] M. R. Portnoff, "Time-frequency representation of digital signals and systems based on short-time Fourier analysis," *IEEE Trans. Acoust., Speech, Signal Processing*, vol. ASSP-28, pp. 55–69, 1980.

[26] M. Zibulski and Y. Y. Zeevi, "Discretization of the Gabor-type scheme by sampling of the Zak transform," in *Proc. SPIE Conf. Visual Commun. Image Processing*, A. K. Katsaggelos, Ed., Chicago, IL, Sept. 1994.

[27] K. Assaleh, Y. Y. Zeevi, and I. Gertner, "On the realization of the Zak–Gabor representation of images," in *Proc. Visual Commun. Image Processing*, Nov. 1991.

[28] N. Polyak, W. A. Pearlman, and Y. Y. Zeevi, "Orthogonalization of circular stationary vector sequences and its application to the Gabor decomposition," *IEEE Trans. Signal Processing*, vol. 43, pp. 1778–1789, Aug. 1995.

[29] J. Wexler and S. Raz, "Gabor representation on nonrectangular grids," EE Pub. 822, Technion—Israel Inst. Technol., Haifa, Feb. 1992.

Meir Zibulski (M'95) received the B.Sc., M.Sc., and Ph.D. degrees, all from the Department of Electrical Engineering, Technion—Israel Institute of Technology, Haifa, in 1989, 1992, and 1996, respectively.

In October 1995, he joined IBM Haifa Research Laboratory, where he is currently involved in speech processing and speech recognition projects. His research interests include signal and image representation in combined spaces, sampling theory, speech recognition, and speech coding.

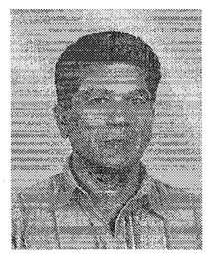

Yehoshua Y. Zeevi received the B.S. degree from the Technion—Israel Institute of Technology, Haifa, the M.Sc. degree from the University of Rochester, Rochester, NY, and the Ph.D. degree from the University of California, Berkeley.

He is the Barbara and Norman Seiden Professor of Computer Sciences and the Dean of the Faculty of Electrical Engineering, Technion—Israel Institute of Technology. He was a Vinton Hayes Fellow at Harvard University, Cambridge, MA, and has been a regular visitor there. He was also a Visiting Professor at the Massachusetts Institute of Technology, Cambridge, and the CAIP Center, Rutgers University, Piscataway, NJ. His major research has been devoted to vision and image sciences and to signal and image representation in combined spaces. He is one of the founders of i Sight, Inc., a company devoted to digital photography and real-time image processing.

Dr. Zeevi is a Fellow of the SPIE and the Rodin Academy, the Editor-in-Chief of the *Journal of Visual Communication and Image Representation* (New York: Academic) and a member of the editorial boards of several journals.